JOURNAL OF APPLIED ELECTROCHEMISTRY **27** (1997) 497–506

Mechanism of hydrogen oxidation on a platinum-loaded gas diffusion electrode

J. J. T. T. VERMEIJLEN[*], L. J. J. JANSSEN[*‡], G. J. VISSER[§]

Eindhoven University of Technology, [*]Laboratory of Instrumental Analysis, Department of Chemical Engineering and [§]Computing Center, P.O. Box 513, 5600 MB Eindhoven, The Netherlands

Received 7 December 1995; revised 10 August 1996

The mechanism of hydrogen oxidation on a platinum-loaded gas-diffusion electrode has been investigated. Experimental potential–current curves, especially in the low overpotential range, have been measured for H_2–N_2 mixtures with a small content of hydrogen and for pure H_2. Theoretical relations have also been presented. Comparing the experimental and theoretical relations, it is concluded that the hydrogen oxidation occurs according to the Volmer–Tafel mechanism. The reactivity of the electrode has a large effect on the kinetic parameters for hydrogen oxidation. The limiting current is determined by diffusion of hydrogen for a very reactive gas diffusion electrode and by the Tafel reaction for a gas diffusion electrode with a low reactivity. The transfer coefficient for the Volmer reaction α_V is 0.5 and $i_{0,V}/i_{0,T} \leq 0.1$ for a very reactive gas diffusion electrode. α_V increases and $i_{0,V}/i_{0,T}$ ratio decreases with decreasing reactivity of the gas diffusion electrode.

List of symbols

c	concentration (mol m^{-3})
E	electrode potential (V)
E_0	equilibrium electrode potential at standard conditions (V)
f	constant at constant temperature, $f = \mathscr{F}/RT$
$\mathscr{F}$	Faraday constant (96 500 A s mol^{-1})
i	current density (A m^{-2})
k	reaction rate constant
k_d	diffusion rate constant
R	gas constant, $R = 8.314$ J K^{-1} mol^{-1}
R_{ct}	charge transfer resistance (Ω m^2)
T	temperature (K)
y	parameter defined in Section 4

Greek letters

α	transfer coefficient
θ	fractional surface coverage
η	overpotential (V), $\eta = E - E_r$

Subscripts

a	anodic
b	bulk of solution, bulk of gas
c	cathodic
d	diffusion
in	at the inlet of the gas compartment
l	limited
out	at the outlet of the gas compartment
r	under reversible conditions
s	surface, solution
T	Tafel reaction
V	Volmer reaction
VT	Volmer–Tafel reactions
0	exchange

Superscripts

ref	reference conditions, $\theta^{ref} = 0.5$
$*$	at $E_r = 0$ V
$\prime$	forward reaction (Tafel mechanism)

1. Introduction

Despite the importance of the hydrogen oxidation reaction on platinum in acidic solution (e.g., in fuel cells), this process has been investigated less than the hydrogen evolution process. Short reviews on hydrogen oxidation by Vetter [1], Breiter [2] and Appleby *et al.* [3] are examples in the literature. The results obtained with rotating disc experiments depend strongly on how the platinum electrode is activated [4]. Harrison and Khan [5] showed the presence of diffusion control even at very high angular velocities for an active platinum electrode. In the overpotential region where platinum is covered with oxygen or an oxide layer, the hydrogen oxidation limiting current is much lower than its limiting diffusion current [6]. Rotation rate independent limiting currents have also been obtained for inactive platinum in the low overpotential range, that is, for $\eta < 0.1$ V [7]. In this case, the overpotential–current density relation is explained using the Volmer–Heyrowsky mechanism where adsorption of molecular hydrogen is the rate determining step [1].

‡ Author to whom correspondence should be sent.

0021-891X

Results for platinum and platinized platinum obtained by Volmer and Wick [8] and by Roiter and Polujan [9] have been described by equations for the Volmer–Tafel mechanism [1]. This mechanism is also used by Vogel *et al*. [10] and Stonehart and Ross [11] for hydrogen oxidation at platinum catalysed gas diffusion electrodes in concentrated phosphoric acid at high temperatures.

Based on a high Tafel slope Couturier *et al*. [12] have predicted that the mechanism of the hydrogen oxidation reaction on platinum is a fast dissociative adsorption of molecular hydrogen Tafel reaction followed by slow ionization of adsorbed atomic hydrogen (Volmer reaction). The authors, have stated that additional work is necessary to be more certain of the mechanism.

In this work, experimental potential–current density curves for gas diffusion electrodes (GDEs) with various reactivities are presented for various hydrogen concentrations in the feed gas of the GDE. Experiments were carried out in dilute sulfuric acid at low temperatures. To establish the mechanism of hydrogen oxidation, theoretical relations for various mechanisms with various rate-determining steps are compared with the experimental results.

2. Experimental details

The experimental cell is shown in Fig. 1 and is described in detail elsewhere [12]. The cell was fitted with fuel cell grade electrodes on Toray paper containing 0.50 mg cm^{-2} Pt (E-TEK, USA). A geometric surface area of 20 mm × 20 mm of the electrode was exposed to gas and solution.

The solution used was 0.5 M H_2SO_4 prepared from 95–97% sulfuric acid (Merck) and deionized water. The solution was recirculated through the solution compartment of the test cell at a rate of 5 cm^3 s^{-1}. A heat exchanger near the solution inlet of the test cell was used to keep the solution, as well as the test cell, at a constant temperature of 298 K. The test cell was fitted with a platinum counter electrode. A saturated calomel electrode (SCE) was connected to the Luggin capillary and served as reference electrode.

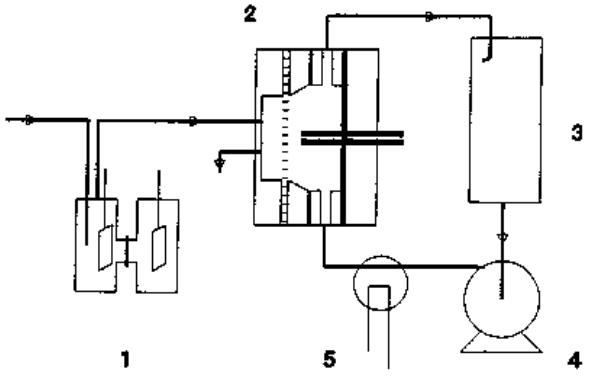

Fig. 1. Schematic illustration of the experimental setup. (1) Hydrogen generation cell, (2) gas diffusion electrode test cell, (3) solution storage vessel, (4) pump and (5) heat exchanger.

For measurements with low hydrogen concentrations, hydrogen was generated from a 4 M KOH solution in an electrochemical H-cell fitted with a Nafion® ion-exchange membrane. The hydrogen generated was added to a nitrogen stream. The gas mixture was fed to the inlet of the gas compartment of the test cell. The nitrogen stream was kept at a constant volumetric flow rate of 5.08 cm^3 s^{-1}. For measurements with pure hydrogen, hydrogen was passed to the experimental cell at a volumetric flow rate of 5.08 cm^3 s^{-1} from a gas cylinder.

To activate new electrodes, an anodic current of 2.5 kA m^{-2} was applied to the test cell while nitrogen was passed through the gas compartment. This current was maintained for 30 min to oxidize pollutants from the electrocatalytic surface. Afterwards, the working electrode was set to a potential of approximately −0.2 V vs SCE to reduce the platinum oxides. Hydrogen was added to the nitrogen stream. The diffusion limited current was determined to gain an insight into the activity of the gas diffusion electrode.

Generally, voltammograms were recorded using an Eco Chemie PGSTAT 20 Autolab controlled by a microcomputer. The potential was scanned over a range of 400 mV in steps of 1 or 5 mV s^{-1} and over 15 mV in steps of 0.1 mV s^{-1}. Voltammograms were also measured using a Solartron 1286 electrochemical interface (ECI) or a Wenking POS73 potentioscan. Potentials used in this work are referred to the potential of the saturated calomel electrode (SCE).

The ohmic potential drop between the working electrode and the tip of the Luggin capillary was determined from the electrochemical impedance spectra. These spectra were recorded using the Solatron 1286 electrochemical interface combined with a Solartron 1250 frequency response analyser. Moreover, the current interruption technique was also used to determine the ohmic potential drop. Electrode overpotentials were corrected for ohmic potential drop.

3. Theory

The most extensively investigated electrode reaction is probably the hydrogen evolution reaction. The hydrogen oxidation reaction has been studied much less [1]. This discussion assumes an acidic solution. In this medium the overall reaction equation for hydrogen oxidation is expressed by

$$H_2 \rightarrow 2H^+ + 2e^- \quad (1)$$

Generally, the following mechanisms are proposed for this reaction.

(i) the Volmer–Tafel mechanism:

$$H_2 \rightarrow 2H_{ad} \quad \text{(Tafel reaction)} \quad (2)$$

and

$$H_{ad} \rightarrow H^+ + e^- \quad \text{(Volmer reaction)} \quad (3)$$

(ii) the Volmer–Heyrowsky mechanism:

$$H_2 \rightarrow H_{ad} + H^+ + e^- \quad \text{(Heyrowsky reaction)} \quad (4)$$

and

$$H_{ad} \rightarrow H^+ + e^- \quad \text{(Volmer reaction)} \qquad (3)$$

Some investigators have proposed another mechanism for hydrogen oxidation [13] which may be represented by

$$H_2 \rightarrow H_2^+ + e^- \qquad (5)$$

$$H_2^+ \rightarrow H^+ + H_{ad} \qquad (6)$$

$$H_{ad} \rightarrow H^+ + e^- \qquad (3)$$

It was shown that this mechanism is not thermodynamically feasible [14].

Assuming that the fractional coverage of the electrode surface by adsorbed hydrogen atoms is given by the Langmuir isotherm, the rate equations for Reactions 2–4 are well known [1]. The current density for the Volmer reaction, i_V, is given by

$$i_V = \mathscr{F} k^*_{a,V} \theta \exp(\alpha_V f E) - \mathscr{F} k^*_{c,V} c_{H^+,s}(1-\theta) \exp(-(1-\alpha_V) f E) \qquad (7)$$

The rate for the Tafel reaction is denoted by the current density i_T. The electronation current density i_T is given by

$$i_T = 2\mathscr{F} k'_T c_{H_2,s} (1-\theta)^2 - 2\mathscr{F} k_T \theta^2 \qquad (8)$$

The current density for the Heyrowsky reaction is given by

$$i_H = \mathscr{F} k^*_{a,H} (1-\theta) c_{H_2,s} \exp(\alpha_H f E) - \mathscr{F} k^*_{c,H} c_{H^+,s} \theta \exp(-(1-\alpha_H) f E) \qquad (9)$$

The mass transfer rate for the dissolved molecular hydrogen to a plane electrode is indicated by the electronation current density i_d, where i_d is given by

$$i_d = 2\mathscr{F} k_d (c_{H_2,b} - c_{H_2,s}) \qquad (10)$$

Since the diffusion limiting electronation current density is

$$i_{d,l} = 2\mathscr{F} k_d c_{H_2,b} \qquad (11)$$

and moreover, since $i = i_d$, it can be deduced that

$$c_{H_2,s} = \frac{i_{d,l} - i}{2\mathscr{F} k_d} \qquad (12)$$

In the following Sections it is assumed that no concentration polarization for H^+ occurs, so that $c_{H^+,b} = c_{H^+,s} = c_{H^+,r}$. The reversible potential at a hydrogen pressure of 1 atm, denoted by E_0, is used as reference potential.

In the gas diffusion electrode, hydrogen gas is transferred from the gas phase into the liquid phase. The concentrations of hydrogen on both sides of the gas–liquid interface are in equilibrium and linked by means of the Henry coefficient, H. Since in all relations the hydrogen surface concentration can be made large, gas phase concentrations are used. It should be noted that k_d or k_T are, in effect, the product H and the respective parameter. Relations between current density and electrode potential have been calculated for both the Volmer–Tafel and the Volmer–Heyrowsky mechanism [15]. In this paper, only the Volmer–Tafel mechanism is extensively discussed. It was found that the Volmer–Heyrowsky mechanism may be excluded [15].

3.1. *Volmer–Tafel mechanism*

The total current density for hydrogen oxidation $i = i_V = i_T$. At the equilibrium potential E_r at $c_{H_2,r}$ and $c_{H^+,r}$, the anodic and cathodic currents must sum to zero. Therefore, in this case, the rate of the recombination Tafel reaction is that of the dissociative Tafel reaction and the rate of the anodic Volmer reaction is that of the cathodic Volmer reaction. From these equalities, it can be deduced that

$$k_T = \frac{c_{H_2,r} (1-\theta_r)^2 k'_T}{\theta_r^2} \qquad (13)$$

and

$$k^*_{c,V} = \frac{k^*_{a,V} \theta_r \exp(f E_r)}{(1-\theta_r) c_{H^+,r}} \qquad (14)$$

From Equations 8, 12 and 13 it follows that

$$i = \frac{\frac{(1-\theta)^2}{(1-\theta_r)^2} - \frac{\theta^2}{\theta_r^2}}{\frac{1}{i_{0,T}} + \frac{1}{i_{d,l}} \frac{(1-\theta)^2}{(1-\theta_r)^2}} \qquad (15)$$

where $i_{0,T} = 2\mathscr{F} k'_T c_{H_2,r} (1-\theta_r)^2 \qquad (16)$

The limiting current density for the H_2 oxidation determined by the Tafel reaction only is given by

$$i_l = i_{T,l} = 2\mathscr{F} k'_T c_{H_2,r} \qquad (17)$$

and that determined by both the Tafel reaction and the hydrogen diffusion is

$$i_l = \frac{i_{T,l} \times i_{d,l}}{i_{T,l} + i_{d,l}} = \frac{2\mathscr{F} k'_T k_d}{k'_T + k_d} c_{H_2,r} \qquad (18)$$

From this result it can be seen that i_l is always proportional to $c_{H_2,r}$, independent of diffusion or reaction being the rate controlling process.

The relation between current density i and electrode potential E is given by the Volmer reaction. After introducing

$$k_{a,V} = k^*_{a,V} \exp(\alpha_V f E_r) \qquad (19)$$

into Equation 7, and using Equations 7 and 14, we obtain

$$i = i_{0,V} \left[\frac{\theta}{\theta_r} \exp(\alpha_V f \eta - \frac{(1-\theta)}{(1-\theta_r)} \exp(-(1-\alpha_V) f \eta) \right] \qquad (20)$$

where $i_{0,V} = \mathscr{F} k_{a,V} \theta_r \qquad (21)$

For hydrogen oxidation according to the Volmer–Tafel mechanism, the relations between i, θ_r and η were calculated using Equations 15–18 and 20 for $\alpha_V = 0.5$, $f = 38.94\,V^{-1}$ being the factor $RT/\mathscr{F}$ at 298 K, $i_{d,l}/i_{T,l}$ from 10^4 to 10^{-2}, $i_{0,V}/i_{0,T}$ from 10^3 to 10^{-3}, $\theta_r = 0.01,\ 0.1,\ 0.5,\ 0.9$ and 0.99 and $i_{T,d,l} = 0.2$ and $20\,kA\,m^{-2}$.

These calculations also involve the extreme cases, with diffusion of molecular hydrogen, Tafel reaction

or Volmer reaction as the rate-determining step. The results calculated can be presented using different relationships. Which relationship is chosen depends on the rate-determining step discussed.

In the case where the diffusion of hydrogen solely determines the polarization curve, then $i_{0,T}$ and $i_{0,V} \gg i_{d,l}$. From Equations 15 and 20 it was found that $(i_{d,l} - i)/i_{d,l} = \exp(-2f\eta)$ and $i \approx i_{d,l}$ at $\eta = 0.06\,V$. This relationship has been given in [1].

If the Tafel reaction completely determines the polarization curve, then $i_{0,T} \ll i_{d,l}$ and $i_{0,T} \ll i_{0,V}$. The Volmer reaction may be treated as an equilibrium. From Equation 20, it can be deduced that

$$\frac{\theta}{\theta_r} = \frac{1-\theta}{1-\theta_r}\exp(-f\eta) \qquad (22)$$

The limiting current density [1] is given by

$$i_{T,l} = \frac{i_{0,T}}{(1-\theta_r)^2} \qquad (23)$$

The relation between i and η can be calculated using Equations 15, 23 and 24, $f = 38.94\,V^{-1}$ and various θ_r, $i_{0,T}$ if $i_{d,l} \gg i_{T,l}$. Characteristic results are shown in [1]. For low θ_r, viz. $\theta_r \leq 0.1$, the limiting current density is almost reached at low overpotentials, that is, $\eta \leq 0.05\,V$, and for $\theta_r = 0.9$ a limiting current density was obtained at $\eta \approx 0.120\,V$.

In the case where the Volmer reaction is the unique rate-determining step, no limiting current density occurs and the Tafel reaction is at quasi-equilibrium, where $i_{0,T} \to \infty$. Using this assumption, it can be found that $\theta \approx \theta_r$ and the i–η curve is given by

$$i = i_{0,V}\{\exp(\alpha_V f\eta) - \exp(-(1-\alpha_V)f\eta)\} \qquad (24)$$

Some extreme cases were previously discussed. The polarization curve can be affected by more than one step; there is no unique rate-determining step. To obtain a straight line over a wide range of overpotentials [1], the expression

$$\log\frac{i}{i_{0,VT}} - \log\left[\left[\frac{i_{d,l}-i}{i_{d,l}}\right]^{1/2} - \exp(-f\eta)\right]$$

is plotted against overpotential (η), where $i_{0,VT} = (i_{0,V} \times i_{0,T})/(i_{0,V} + i_{0,T})$. From the corrected Tafel slope, the transfer coefficient α_V can be determined. Characteristic results are represented as modified Tafel plots in Figs 2–4 to show the effect of $i_{0,V}/i_{0,T}$, θ_r and $i_{d,l}/i_{T,l}$, respectively. The curves

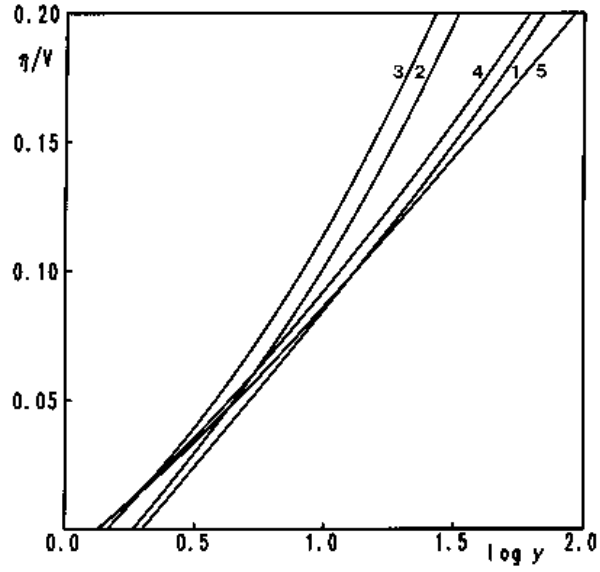

Fig. 3. log y is plotted against η where $y = i/[i_{0,VT}[((i_{d,l}-i)/i_{d,l})^{0.5} - \exp(-f\eta)]]$ for hydrogen oxidation according to the Volmer–Tafel mechanism at $i_{T,l} = 2 \times 10^{-2}\,A\,m^{-2}$, $i_{d,l}/i_{T,l} = 10, i_{0,V}/i_{0,T} = 1, \alpha_V = 0.5, f = 38.94\,V^{-1}$ and various θ_r ratios: 0.01 (1), 0.1 (2), 0.5 (3), 0.9 (4) and 0.99 (5).

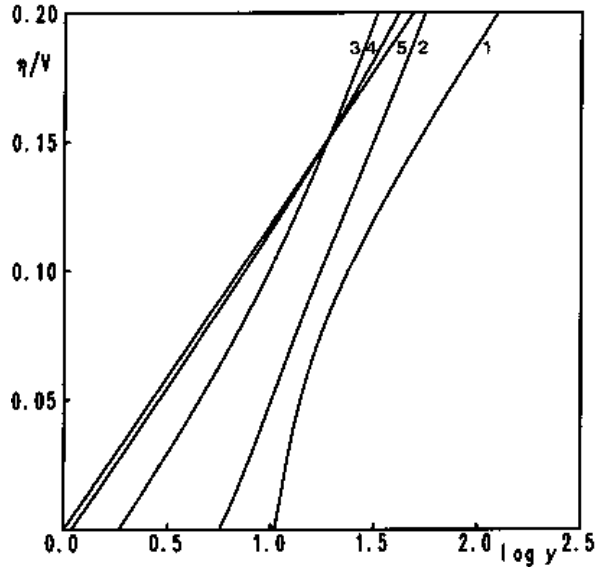

Fig. 2. log y is plotted against η where $y = i/[i_{0,VT}[((i_{d,l}-i)/i_{d,l})^{0.5} - \exp(-f\eta)]]$ for hydrogen oxidation according to the Volmer–Tafel mechanism at $i_{T,l} = 2\,times\,10^{-2}\,A\,m^{-2}$, $i_{d,l}/i_{T,l} = 10, \theta_r = 0.1, \alpha_V = 0.5, f = 38.94\,V^{-1}$ and various $i_{0,V}/i_{0,T}$ ratios: 10^3 (1), 10 (2), 1 (3), 10^{-1} (4) and 10^{-3} (5).

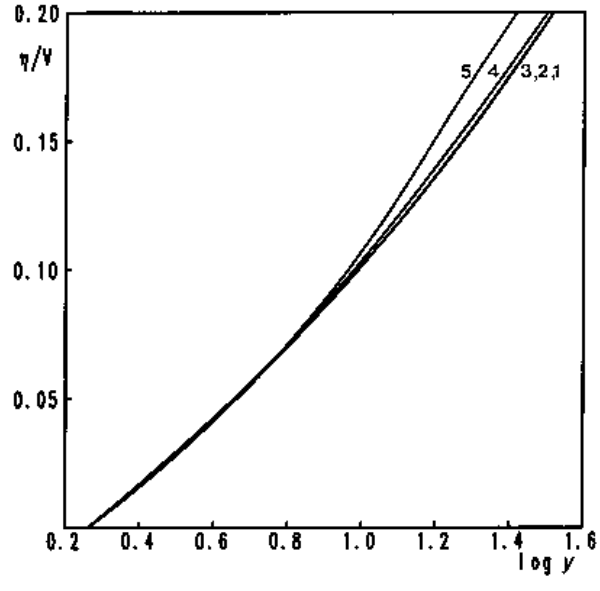

Fig. 4. log y is plotted against η where $y = i/[i_{0,VT}[((i_{d,l}-i)/i_{d,l})^{0.5} - \exp(-f\eta)]]$ for hydrogen oxidation according to the Volmer–Tafel mechanism at $i_{d,l} = 2 \times 10^{-2}\,A\,m^{-2}$, $i_{0,V}/i_{0,T} = 1$, $\theta_r = 0.1, \alpha_V = 0.5, f = 38.94\,V^{-1}$ and various $i_{d,l}/i_{T,l}$ ratios: 10^4 (1), 10 (2), 1 (3), 10^{-1} (4) and 10^{-2} (5).

intersect the horizontal axis at various points due to neglecting the effect of θ terms.

From Figs 2–4 it follows that the corrected Tafel slope strongly depends on the three parameters $i_{0,V}/i_{0,T}$, θ_r and $i_{d,l}/i_{T,l}$. A corrected Tafel slope of almost 2.3 $(\alpha f)^{-1}$, being 118 mV at 298 K and for $\alpha_V = 0.5$, has been found for $i_{0,V}/i_{0,T} < 10^{-1}$ and for the θ_r range from 0.01 to 0.99. Moreover, in the $i_{0,V}/i_{0,T}$ range from 10^{-1} to 10 the corrected Tafel slope decreases with increasing overpotential. This decrease depends on $i_{0,V}/i_{0,T}$, θ_r and $i_{d,l}/i_{T,l}$. From the results calculated it was also found that the corrected Tafel slope does not depend on $i_{T,l}$.

Enyo [16] has extensively discussed the Volmer–Tafel mechanism with no unique rate–determining step. For the case where more steps are not in quasi-equilibrium, he pays attention to the distribution of the affinity of the overall reaction among the steps involved. Enyo has split the overpotential η into the component overpotentials η_V and η_T for the Volmer and Tafel reaction, respectively. Calculations have shown that η_T increases at a decreasing rate and η_V increases at an increasing rate with increasing η. The effect of the Tafel reaction on the polarization curve decreases with increasing overpotential.

3.2. *Effect of hydrogen concentration on the charge transfer resistance for the Volmer–Tafel mechanism*

The charge transfer resistance, R_{ct}, is defined as the reverse of the slope of the polarization curve [1]:

$$R_{ct} = \left[\frac{d\eta}{di}\right]_{\eta=0} \tag{25}$$

To elucidate the influences of bulk hydrogen concentration, the current–overpotential relations for low overpotentials, that is, $\eta < 10$ mV, are calculated for the Volmer–Tafel and the Volmer–Heyrowsky mechanism. Only the results for the Volmer–Tafel mechanism are reported in this paper. Again, the proton concentration polarization is assumed absent, so c_{H^+} is assumed constant. Also, the influence of hydrogen diffusion is neglected since the overpotentials under consideration are very low. As a reference condition, $\theta_r^{ref} = 0.5$ is introduced.

This reference surface coverage is reached at $c_{H_2,r} = c_{H_2,r}^{ref}$. From Nernst's law [1]

$$E_r^{ref} - E_r = \frac{1}{2f} \ln \frac{c_{H_2,r}}{c_{H_2,r}^{ref}} \tag{26}$$

For the equilibrium of the Volmer reaction under reversible conditions and reversible reference conditions, it can be derived from Equation 7 and using $\theta_r^{ref} = 0.5$ that

$$\frac{\theta_r}{1-\theta_r} = \exp(f(E_r^{ref} - E_r)) \tag{27}$$

The exchange current densities for the Volmer and the Tafel reaction as a function of $[c_{H_2,r}/c_{H_2,r}^{ref}]$ are estimated as described below. For the Volmer reaction,

$$\frac{i_{0,V}}{i_{0,V}^{ref}} = \frac{\theta_r}{\theta_r^{ref}} \left[\frac{c_{H_2,r}}{c_{H_2,r}^{ref}}\right]^{-\alpha_V/2} \tag{28}$$

and, for the Tafel reaction,

$$\frac{i_{0,T}}{i_{0,T}^{ref}} = \frac{c_{H_2,r}}{c_{H_2,r}^{ref}} \frac{(1-\theta_r)^2}{(1-\theta_r^{ref})^2} \tag{29}$$

The relation between θ_r and $c_{H_2,r}$ can be derived from Equations 26 and 27 and is given by

$$\frac{\theta_r}{1-\theta_r} = \frac{\theta_r^{ref}}{1-\theta_r^{ref}} \frac{c_{H_2,r}^{0.5}}{\left(c_{H_2,r}^{ref}\right)^{0.5}} \tag{30}$$

The relation between $i_{0,VT}/i_{0,VT}^{ref}$ and $c_{H_2,r}/c_{H_2,r}^{ref}$ has been calculated for $\alpha_V = 0.5$, $\theta_r^{ref} = 0.5$ at $c_{H_2,r}^{ref}$ and selected values of $i_{0,V}^{ref}$ and $i_{0,T}^{ref}$. Results are presented on a double logarithmic scale in Fig. 5. Calculations were also carried out for $\alpha_V = 0.5$ and constant $i_{0,V}^{ref}/i_{0,T}^{ref}$ ratio's and corresponding values for $i_{0,V}^{ref}$ and $i_{0,T}^{ref}$ and for $\alpha_V = 0.2$, 0.3, 0.4 and 0.5 at $i_{0,V}^{ref}/i_{0,T}^{ref} = 1$, 0.1 and 0.01. It was found that the $\log(i_{0,VT}/i_{0,VT}^{ref}) - \log(c_{H_2,r}/c_{H_2,r}^{ref})$ curve at $\alpha_V = 0.5$ depends only on the $i_{0,V}^{ref}/i_{0,T}^{ref}$ ratio. The effect of α_V on this curve is determined by the $i_{0,V}^{ref}/i_{0,T}^{ref}$ as well as the $c_{H_2,r}/c_{H_2,r}^{ref}$ ratio.

For the Volmer–Tafel mechanism the charge transfer resistance $R_{ct} = (i_{0,VT}f)^{-1}$ [1]. For the selected values of $i_{0,V}^{ref}$ and $i_{0,T}^{ref}$ from Fig. 5 the polarization curves for the Volmer–Tafel mechanism have been calculated as a function of $c_{H_2,r}/c_{H_2,r}^{ref}$. These calculations have shown that the polarization curves

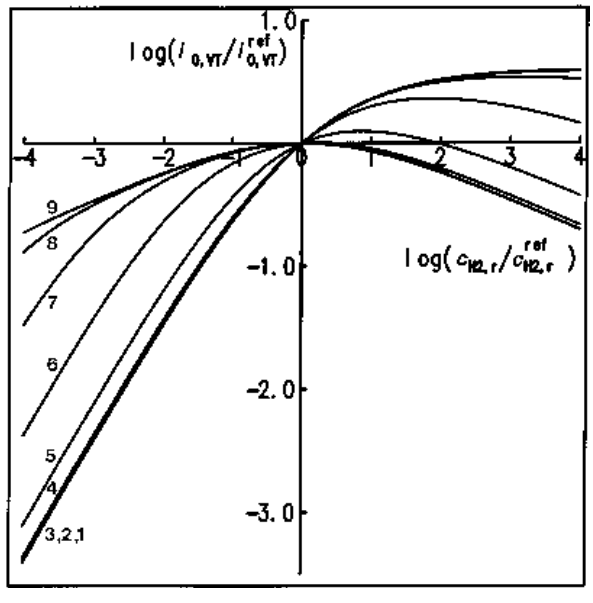

Fig. 5. The calculated ratio $i_{0,VT}/i_{0,VT}^{ref}$ is plotted against the hydrogen concentration ratio, $c_{H_2,r}/c_{H_2,r}^{ref}$ on a double-logarithmic scale for the Volmer–Tafel mechanism. $f = 38.94\,V^{-1}$, $\alpha_V = 0.5$ and various exchange current densities at reference conditions, $i_{0,V}^{ref}$ and $i_{0,T}^{ref}$: 10^4 and 10^0 (1), 10^4 and 10^1 (2), 10^4 and 10^2 (3), 10^4 and 10^3 (4), 10^4 and 10^4 (5), 10^3 and 10^4 (6), 10^2 and 10^4 (7), 10^1 and 10^4 (8), 10^0 and 10^4 (9) A m^{-2}, respectively.

are practically straight lines up to overpotentials of approximately 15 mV.

4. Results

Preliminary experiments showed that the reactivity of a platinum-loaded gas-diffusion electrode (GDE) strongly depends on its pretreatment; in particular, anodic polarization succeeded by cathodic polarization enhances its electrocatalytic activity towards hydrogen oxidation.

To investigate accurately the effect of hydrogen concentration on the polarization behaviour of a GDE, its electroactivity has to be constant during a series of experiments. Hence, special attention was paid to the experimental conditions during a series of experiments. The potential was cycled over 400 mV to determine the limiting current for hydrogen oxidation and over 15 mV to determine the charge transfer resistance. Figure 6 shows the voltammograms for the first, second, fourth and eleventh cycle over 400 mV for a fresh GDE electrode, where the first, second and eleventh cycle were measured at $c_{H_2,in} = 41\,mol\,m^{-3}$ (pure hydrogen) and the fourth cycle at $c_{H_2,in} = 4.55\,mol\,m^{-3}$. The potentials are not corrected for the ohmic potential drop in the solution. The ohmic resistance between the working electrode and the tip of the Luggin capillary was 0.09 Ω.

The first cycle over 400 mV was carried out after a half-hour nitrogen gas and a one-hour H_2 gas passage through the gas compartment of the cell, where the GDE was on open-circuit, and after four cycles over a potential range of 15 mV.

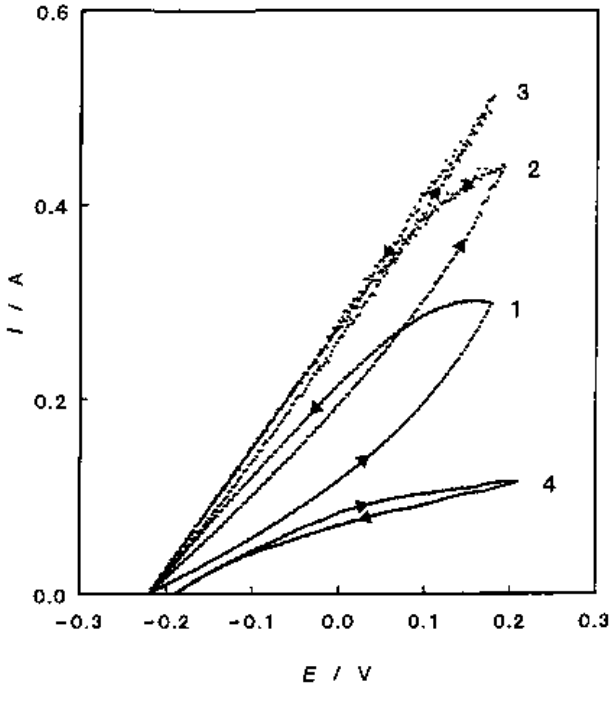

Fig. 6. Voltammograms in a series of experiments for the hydrogen oxidation on a fresh gas diffusion electrode at a gas inlet of pure hydrogen (first voltammogram: (1), second (2) and eleventh (3)) and of a H_2–N_2 mixture containing 4.55 mol m^{-3} H_2 (4). Data were not corrected for the ohmic potential drop.

To determine the charge transfer resistance R_{ct} in the periods between subsequent cycles over 400 mV, four cycles over 15 mV were carried out. After each cycle over 400 mV from the second the hydrogen concentration in the gas feed was decreased in steps from 41 to 0.32 mol m^{-3} and thereafter increased also in steps to 41 mol m^{-3}.

From Fig. 6 it follows that for $c_{H_2,in} = 41\,mol\,m^{-3}$ the current density during the anodic sweep is lower than that during the cathodic sweep and their difference becomes smaller with increasing number of 400 mV cycles. It was found that the hysteresis behaviour at low hydrogen concentrations is opposite to that with pure hydrogen. The limiting current density decreased and the modified Tafel slope increased slightly for subsequent voltammograms over 400 mV at $c_{H_2,in} = 1.25\,mol\,m^{-3}$ during the part of the series of experiments where the hydrogen concentration decreased.

The measuring points were scattered in a zone widening with increasing current; (see Fig. 4.10 from [15]). Current oscillations with an asymmetric shape and a frequency of about 0.013 s^{-1} were observed for the three different techniques used to measure the potential–current curves. It was found that these oscillations are not caused by solution pumping through the cell and gas bubbling through the solution in the vessel placed in the gas circuit after the cell. These oscillations were not related to electrode potentials. It is likely that the current oscillations are related to alterations in the position of the liquid–gas boundary surface inside the GDE and/or to changes of the electroactivity of GDE. The cause of these changes is unknown.

The curve for $c_{H_2,in} = 4.55\,mol\,m^{-3}$ given in Fig. 6 shows these oscillations. The effect of the oscillations on the potential–current curve increases with decreasing $c_{H_2,in}$. Hence, the determination of the slope of the potential–current curve at low hydrogen concentrations was strongly impeded by the asymmetric oscillations. To obtain reliable results for the charge transfer resistance, four cycles over 15 mV were carried out for each hydrogen concentration.

GDEs with strongly different reactivities were used. The reactivity of GDE depends on the conditions of pretreatment, especially the potential during anodic polarization and the time of anodic polarization. The current density at a fixed overpotential can be used as a measure of its reactivity. In this work the lowest and the highest current density for GDEs fed with pure hydrogen gas and at an overpotential of 60 mV were 0.35 and 1.72 kA m^{-2}, respectively. Vermeijlen [15] has used a GDE with a higher reactivity.

Taking into account the consumption of hydrogen at the limiting current, the concentration of hydrogen at the outlet of the gas compartment $c_{H_2,out}$ can be calculated. Since the gas compartment behaves like a continuously fed stirred tank reactor [12] the concentration of hydrogen in the gas compartment of the cell $c_{H_2,b} = c_{H_2,out}$. It was found that for GDEs with a

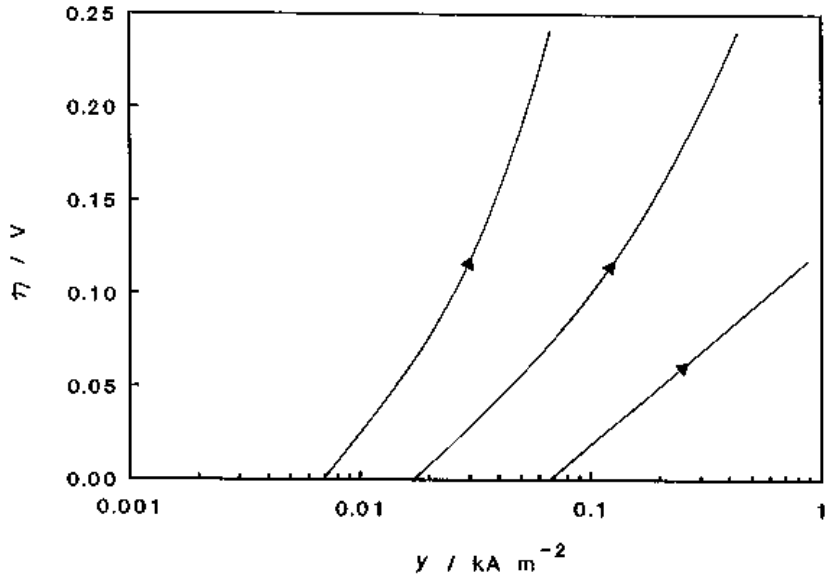

Fig. 7. The current density is plotted against $\log y$, where $y = i/\left[i_{0,\mathrm{VT}}\left[((i_{\mathrm{d,l}} - i)/i_{\mathrm{d,l}})^{0.5} - \exp(-f\eta)\right]\right]$ and $f = 38.94\,\mathrm{V}^{-1}$ for GDEs with different reactivities at a gas inlet of pure hydrogen. The arrow on the curve indicates the direction of the potential scan.

small reactivity i_{l} is practically proportional to $c_{\mathrm{H_2,b}}$. This result is also given in [15]. For the most reactive GDE at low $c_{\mathrm{H_2,in}}$ the limiting current is practically equal to the current for the hydrogen gas production in the hydrogen generation cell; so that $c_{\mathrm{H_2,out}}$ is practically zero and the limiting current can be considered as the diffusion-limited current. It was shown that for very reactive electrodes fed with dilute hydrogen gas the current density plateau at overpotentials over approximately 0.3 V is probably completely diffusion limited, because of the large effect of the nature of the inert gas present in the feed gas for the GDE [17]. Further treatments of activation to obtain a higher limiting current were unsuccessful.

Generally, no limiting current was found for pure hydrogen as gas feed for the GDE. The limiting current for pure hydrogen was calculated from the one at the highest hydrogen concentration where still a limiting current was found.

To obtain kinetic parameters for the hydrogen oxidation, the overpotential η is plotted against y on a semilogarithmic scale, where $y = i/[((i_{\mathrm{l}} - i)\ /i_{\mathrm{l}})^{0.5} - \exp(-f\eta)]$. and $f = 38.94\,\mathrm{V}^{-1}$. A similar relation has been plotted in Figs 2–4. Results for GDEs with different reactivities and for pure hydrogen gas as GDE feed are given in Fig. 7 and for a GDE with a relatively low reactivity and for different hydrogen concentrations in Fig. 8.

For GDEs with increasing reactivity, for which results are given in Fig. 7, the limiting current densities for $c_{\mathrm{H_2,in}} = 0.64\,\mathrm{mol\,m^{-3}}$ were 0.68, 0.099 and $0.045\,\mathrm{kA\,m^{-2}}$, where $c_{\mathrm{H_2,b}} \approx 0$, 0.53 and

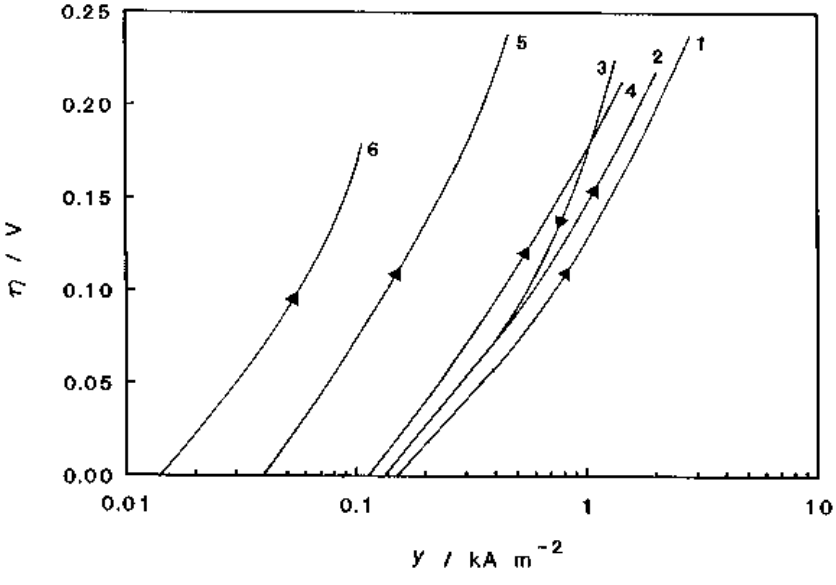

Fig. 8. The current density is plotted against $\log y$, where $y = i/\left[i_{0,\mathrm{VT}}\left[((i_{\mathrm{d,l}} - i)/i_{\mathrm{d,l}})^{0.5} - \exp(-f\eta)\right]\right]$ and $f = 38.94\,\mathrm{V}^{-1}$ for a GDE at a H_2–N_2 mixture containing various hydrogen concentrations: 41 (1), 13.5 (anodic scan: 2; cathodic scan: 3), 4.55 (4), 1.24 (5) and 0.32 (6) $\mathrm{mol\,m^{-3}}$. The arrow on the curve indicates the direction of the potential scan.

$0.59\,\mathrm{mol\,m^{-3}}$, respectively, and those for $c_{H_2,in} = 41\,\mathrm{mol\,m^{-3}}$ were larger than 40, 6.5 and $3.3\,\mathrm{kA\,m^{-2}}$.

From Figs 7 and 8 it follows that the modified Tafel slope increases with decreasing reactivity of the GDE and hydrogen concentration. The modified Tafel slope at $\eta > 0.1\,\mathrm{V}$ also depends on the direction of the potential scan (Fig. 8). From the intersection of the modified Tafel curve with the y axis the apparent exchange current density, i_0, being a measure of the reactivity of GDE, can be obtained.

The apparent exchange current densities, i_0, were also determined from i/E relations in the potential range E_r to $E_r + 15\,\mathrm{mV}$. Hysteresis was practically absent in this small potential scan range. This indicates that the nature of the electrochemical surface remains practically constant during the scan over 15 mV. Moreover, it was found that the current for the hydrogen oxidation increases linearly with increasing potential, when taking into account the effect of oscillations.

Different procedures for a series of experiments were used to determine the voltammogram over 15 mV to obtain a constant nature of the GDE surface at different hydrogen concentrations. One has been given above to describe the conditions of the GDE for which results are given in Fig. 6. The other procedure was to maintain the scan range on 15 mV for the whole series of experiments, where the hydrogen concentration was decreased by steps.

From the slope of the linear E/i curve, the charge transfer resistance R_{ct} was determined. Since $R_{ct} = (i_0 f)^{-1}$ and $f = 38.94\,\mathrm{V^{-1}}$ at $T = 298\,\mathrm{K}$, the apparent exchange current density i_0 can be calculated. Figure 9 shows i_0 as a function of hydrogen concentration $c_{H_2,b}$ in the gas compartment of the cell on a double logarithmic scale for GDEs with various reactivities. It can be shown that $c_{H_2,b} \approx c_{H_2,in}$ for the cycles over 15 mV.

Figure 9 shows results for four series of experiments where two were carried out for decreasing as well as increasing $c_{H_2,in}$; and the others only for decreasing $c_{H_2,in}$. From Fig. 9 it follows that practically no hysteresis occurs for a GDE with a relatively high reactivity, the slope of the $\log i_0 / \log c_{H_2,b}$ curve decreases with increasing reactivity and the applied procedure has practically no effect on the slope of the $\log i_0 / \log c_{H_2,b}$ curve.

5. Discussion

The modified Tafel slope of the linear part of the η against $\log y$ curves increases with decreasing reactivity of the GDE and hydrogen concentration $c_{H_2,in}$ (Figs 7 and 8). From the mass transfer coefficient k_d ($= 7.33 \times 10^{-3}\,\mathrm{m\,s^{-1}}$ [17]) it is estimated that the diffusion-limited current density is about $80\,\mathrm{kA\,m^{-2}}$ at $c_{H_2,in} = 41\,\mathrm{mol\,m^{-3}}$. The calculated limiting current density for the most reactive GDE from Fig. 7 is larger than $40\,\mathrm{kA\,m^{-2}}$. Comparing these limiting current densities it follows that, for the most reactive electrode from Fig. 7, the limiting current is determined dominantly by hydrogen diffusion.

For the less reactive GDEs from Fig. 7 it was found that the limiting current densities are much smaller than the diffusion-limited current densities. This means that the limiting current density is determined by a chemical reaction and not an electrochemical reaction. The Heyrowsky reaction can thus be excluded as rate-determining step. In [15] it is clearly shown that the Volmer–Heyrowsky reaction mechanism has to be rejected.

From Fig. 4 it follows that the modified Tafel slope is practically not affected by the $i_{l,d}/i_{l,T}$ ratio. Fig. 2 shows that the modified Tafel slope at $\eta = 0.030\,\mathrm{V}$ is 118 mV at $i_{0,V}/i_{0,T} \leq 0.1$, 130 mV at $i_{0,V}/i_{0,T} = 1$ and larger than 220 mV at $i_{0,V}/i_{0,T} \geq 10$. Moreover, the shape of the curves from Fig. 2 depends on the $i_{0,V}/i_{0,T}$ ratio. The curves at $i_{0,V}/i_{0,T} \leq 1$ show no inflection point and those at $i_{0,V}/i_{0,T} \geq 10$ have an inflection point.

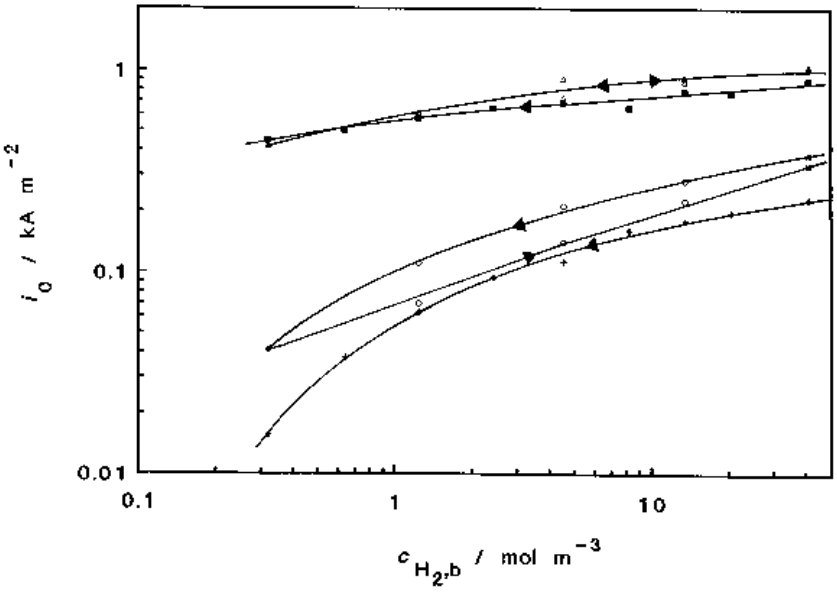

Fig. 9. i_0 against $c_{H_2,b}$ on a double logarithmic scale for GDEs with different reactivities. The arrow on a curve indicates the direction of the concentration change during the series of experiments. Each symbol represents an electrode with a certain reactivity.

For the most reactive GDE, at high as well as low hydrogen concentration, respectively 41 and 0.64 mol m^{-3}, and at $\eta < 100$ mV the modified Tafel slope was 120 mV and the curves can be well described by theoretical curves for $i_{0,V}/i_{0,T} < 1$.

Since for the most reactive GDE at pure hydrogen the current densities at $\eta < 0.1$ V are much smaller than the limiting current, it follows that the degree of coverage θ at $\eta < 0.1$ V is practically equal to θ_r and that the effect of the θ terms on the modified Tafel slope can be neglected. From the modified Tafel slope of 120 mV it is concluded that $\alpha_V = 0.5$. The log i_0/ log $c_{H_2,b}$ curves for the most reactive GDEs are slightly bent, the average slope at $c_{H_2,in} = 5$ mol m^{-3} is 0.15. Comparing this slope with the theoretical ones for the curves from Fig. 5, and taking into account the bending of the experimental and theoretical curves, it can be concluded that the experimental curve can reasonably be described for $i^{ref}_{0,V}/i^{ref}_{0,T} \leq 0.01$ and $c_{H_2,r}/c^{ref}_{H_2,r} \leq 0.37$ at $c_{H_2} = 5$ mol m^{-3}. From this result it follows that $c^{ref}_{H_2,r} \geq 13$ mol m^{-3} where $\theta^{ref}_r = 0.5$. Using Equation 30 and $\theta^{ref}_r = 0.5$, it was calculated that for the most reactive GDE at 41 mol m^{-3} $\theta_r \leq 0.64$.

Consequently, the largest part of the electrochemical surface of the most reactive GDE at pure hydrogen is covered with atomic hydrogen. This result agrees reasonably well with the literature. The degree of coverage of θ_r is very high and even approaches unity for an active platinum electrode in sulfuric acid at 25 °C and at a hydrogen gas pressure of 1 atm [2, 18, 19].

From the results given above, it follows that for the most reactive GDEs used in this work, the hydrogen is oxidized according to the Volmer–Tafel mechanism, where the Volmer reaction is the rate-determining step and $\alpha_V = 0.5$. Practically the same α_V is obtained for the oxidation of hydrogen on a platinum disc in 0.05 M H_2SO_4 from Fig. 208 in [1] for which the same relation is given as in Figs 7 and 8.

Next, the hydrogen oxidation on less reactive GDEs is discussed. The modified Tafel slope is only slightly dependent on the hydrogen concentration (Fig. 8) but depends strongly on the reactivity of GDE (Fig. 7). The reactivity of GDE decreases with increasing number of cycles over 400 mV for low hydrogen concentrations, for instance 1.24 mol m^{-3}. Probably, the hydrogen concentration has only an indirect effect upon the modified Tafel slope. For $c_{H_2,in} = 13.5$ mol m^{-3} Fig. 8 shows that at $\eta > 100$ mV the modified Tafel slope for a cathodic scan is clearly higher than that for an anodic scan and at $\eta < 100$ mV there is practically no difference between the modified Tafel slopes for both scans. The increase in the modified Tafel slope with increasing overpotential (Figs 7 and 8) indicates a change in the nature of the electrochemical surface of the GDE.

From Fig. 6 an opposite hysteresis behaviour at $c_{H_2,in} = 41$ mol m^{-3} is evident. This may be explained by a difference in scan range of the electrode potential for the scan range of 400 mV, due to differences in ohmic potential drop between the tip of the Luggin capillary and the GDE.

The high modified Tafel slope at $\eta = 30$ mV can be explained assuming either $\alpha_V < 0.5$ and $i_{0,V}/i_{0,T} \ll 1$ or $\alpha_V = 0.5$ and $i_{0,V}/i_{0,T} \approx 1$. It was found that the overpotential where the limiting current is reached, increases clearly with decreasing GDE reactivity. This overpotential is practically independent of the hydrogen inlet concentration.

For the most and the least reactive GDE at $c_{H_2,in} = 0.64$ mol m^{-3}, it was found that the overpotentials at $i = 0.95\, i_l$ are 70 and 250 mV, respectively. Calculations showed that this difference corresponds to a factor of about 10 in the $i_{0,V}/i_{0,T}$ ratio; so that $i^{ref}_{0,V}/i^{ref}_{0,T} \leq 0.01$ for the least reactive GDE, since $i^{ref}_{0,V}/i^{ref}_{0,T} \leq 0.1$ for the most reactive GDE. Taking into account that $i_{0,V}/i_{0,T}$ decreases with increasing hydrogen concentration, it follows that the possibility with the conditions $i_{0,V}/i_{0,T} \approx 1$ and $\alpha_V = 0.5$ has to be excluded.

This conclusion is also supported by comparing the experimental log i_0/ log $c_{H_2,b}$ curve and the theoretical log $(i_{0,VT}/i^{ref}_{0,VT})$/ log $c_{H_2,r}/c^{ref}_{H_2,r}$ curves. Assuming $i^{ref}_{0,V}/i^{ref}_{0,T} = 1$ it may be shown that $\theta_r = 0.80$ for the least reactive GDE at $c_{H_2,b} = 41$ mol m^{-3}. This value for θ_r is much too large, since θ_r decreases with decreasing reactivity of platinum [20] being the electrocatalyst of the GDE. From the discussion above it follows that $i^{ref}_{0,V}/i^{ref}_{0,T} \leq 0.01$ for the hydrogen oxidation on the least reactive GDE.

The log i_0/ log $c_{H_2,b}$ curves for less reactive GDEs show a reasonably strong hysteresis. The average slope for the log i_0/ log $c_{H_2,b}$ curves with decreasing $c_{H_2,b}$ and at $c_{H_2,b} = 5$ mol m^{-3} is equal to 0.42. From Fig. 8 it follows that the slope of the η against log y curve at $c_{H_2,b} = 5$ mol m^{-3} and at $\eta < 100$ mV is about 165 mV corresponding to $\alpha_V = 0.4$.

Based on subsequent voltammograms at a low hydrogen concentration and in a series of experiments with decreasing hydrogen concentration, it was concluded that the reactivity of a GDE in steady state decreases with decreasing hydrogen concentration. This means that the reactivity of the GDE is not completely constant during the series of experiments carried out to measure the log i_0/ log $c_{H_2,b}$ relation. Probably, the slope of 0.42 at $c_{H_2,b} = 5$ mol m^{-3} will be maximal.

Analogous to the most reactive GDEs it can be shown that the experimental curve with a slope of 0.42 and $\alpha_V = 0.4$ for the least reactive GDE can reasonably be described for various combinations of $i^{ref}_{0,V}/i^{ref}_{0,T}$ and $c^{ref}_{H_2}$; for instance $i^{ref}_{0,V}/i^{ref}_{0,T} = 0.01$ and $c^{ref}_{H_2} = 1048$ mol m^{-3} corresponding to $\theta_r = 0.16$ at $c_{H_2} = 41$ mol m^{-3}.

Assuming $\alpha_V = 0.4$ and since $\theta^{ref}_r = 0.5$, from Equations 28 and 29 it is derived that

$$\frac{i_{0,V}}{i_{0,T}} = \frac{\theta_r}{2(1-\theta_r)^2}\left[\frac{c_{H_2,r}}{c^{ref}_{H_2,r}}\right]^{-1.20}\frac{i^{ref}_{0,V}}{i^{ref}_{0,T}} \qquad (31)$$

After substitution of θ_r, $c_{H_2,r}/c^{ref}_{H_2,r}$ and $i^{ref}_{0,V}/i^{ref}_{0,T}$ into Equation 31 it was calculated that for the concentration increase from 0.64 to 41 mol m^{-3} $i_{0,V}/i_{0,T}$ decreases from 0.90 to 0.05. Based on the condition $i_{0,V}/i_{0,T} \ll 1$ for the whole range of hydrogen concentration to explain the high modified Tafel slope, it is likely that $i^{ref}_{0,V}/i^{ref}_{0,T} < 0.01$ and $c^{ref}_{H_2} > 1048$ mol m^{-3} for the least reactive electrode.

From the discussion above given for GDEs with a high, as well as a low, reactivity it follows that the hydrogen oxidation occurs according to the Volmer–Tafel mechanism, where the $i_{0,V}/i_{0,T}$ ratio, as well as α_V, decreases with decreasing GDE reactivity. The reactivity of a platinum electrode depends strongly on its electrochemical pretreatment, where potential and time of polarization are significant. Leaving an active platinum electrode at open circuit in electrolytic solutions for days the reactivity of the electrode decreases greatly due to the adsorption of impurities from the electrolyte. The reactivity can be restored by anodic and/or cathodic pretreatment.

References

[1] K. J. Vetter, 'Elektrochemische Kinetik', Springer Verlag, Berlin (1961).
[2] M. W. Breiter, 'Electrochemical Processes in Fuel Cells', Springer Verlag, Berlin (1969).
[3] A. J. Appleby, M. Chemla, H. Kita and G. Bronoël, *in* 'Encyclopedia of Electrochemistry of the Elements' vol. IX, part A (edited by A. J. Bard), Marcel Dekker, New York (1982), pp. 384–97.
[4] V. V. Sobol, A. A. Dmitrieva and A. N. Frumkin, *Soviet Electrochem.* **3** (1976) 928.
[5] J. A. Harrison and Z. A. Khan, *J. Electroanal. Chem.* **30** (1971) 327.
[6] S. Schuldiner, *J. Electrochem. Soc.* **115** (1968) 386.
[7] K. J. Vetter and D. Otto, *Z. Electrochem.* **60** (1956) 1072.
[8] M. Volmer and H. Wick, *Z. Physik Chem.* **172A** (1955) 429.
[9] W. Roiter and J. S. Polujan, *J. Phys. Chem. USSR* **7** (1936) 775.
[10] W. Vogel, J. Lundquist, P. Ross and P. Stonehart, *Electrochim. Acta* **20** (1975) 79.
[11] P. Stonehart and P. N. Ross, *Electrochim. Acta* **21** (1976) 441.
[12] J. J. T. T. Vermeijlen and L. J. J. Janssen, *J. Appl. Electrochem.* **23** (1993) 26.
[13] J. Horiuti, T. Keii and K. Hirota, *J. Res Inst. Catalysis,* Hokkaido University **2** (1950–53) 1.
[14] J. O'M. Bockris and S. Srinivasan, *Electrochim. Acta* **9** (1964) 31.
[15] J. J. T. T. Vermeijlen, Eindhoven, PhD thesis (1994).
[16] M. Enyo, B. E. Conway, J. O'M. Bockris, E. Yeager, S. U. M. Khan and R. E. White (eds), 'Comprehensive Treatise of Electrochemistry', Vol. 7, Plenum Press, New York and London (1983).
[17] J. J. T. T. Vermeijlen and L. J. J. Janssen, *J. Appl. Electrochem.* **23** (1993) 1237.
[18] M. Böld and M. Breiter, *Z. Electrochem.* **64** (1960) 897.
[19] Zh. L. Vert, J. A. Mosevich and J. Tverdovsky, *Doklady Akad. Nuak S.S.S.R.* **140** (1961) 149.